

**Electronic Supplementary Information**

**Understanding of Simultaneous Pyridine and Selenophene-containing Copolymers and their Polarity Conversion in Transistors**

So-Huei Kang,<sup>‡a</sup> Myeonggeun Han,<sup>‡b</sup> Yongjoon Cho,<sup>a</sup> Jisu Hong,<sup>b</sup> Seongmin Heo,<sup>b</sup> Seonghun Jeong,<sup>a</sup> Yong-Young Noh\*<sup>b</sup> and Changduk Yang\*<sup>a</sup>

<sup>a</sup>Department of Energy Engineering, School of Energy and Chemical Engineering, Perovtronic Research Center, Low Dimensional Carbon Materials Center, Ulsan National Institute of Science and Technology (UNIST), 50 UNIST-gil, Ulju-gun, Ulsan 44919, Republic of Korea

<sup>b</sup>Department of Chemical Engineering, Pohang University of Science and Technology (POSTECH), 77 Cheongam-ro, Pohang, Gyeongbuk 37673, Republic of Korea

<b>Table of Contents</b>	<b>Page number</b>
The performances of representative works related to PyDPP-containing and Se-containing polymers	S2–S3
The <sup>1</sup> H and <sup>13</sup> C NMR spectroscopy of the intermediates and polymers	S4–S5
Solubility tests for the polymers	S6
Cyclic voltammograms of the polymers	S7
DFT calculation results of the trimer units	S7
AFM phase images under all annealing conditions	S8
XRD patterns and crystallographic parameters	S9
2D-GIXD crystallographic parameters	S10
FET device results for a low molecular weight P1	S11
References	S12–S13

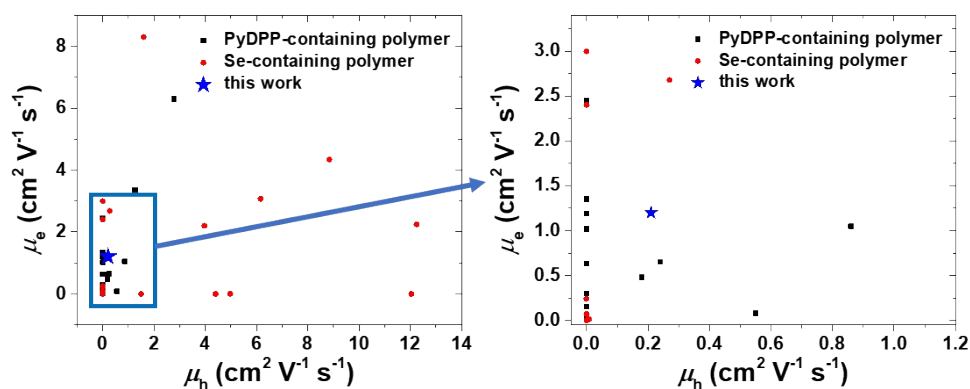


**Chart S1.** The charge carrier transports of PyDPP-containing and Se-containing polymers in OFET devices.

**Table S1.** The charge carrier transports of PyDPP-containing and Se-containing polymers in OFET devices.

Name	unit	$\mu_e$ ( $\text{cm}^2 \text{V}^{-1} \text{s}^{-1}$ )	$\mu_h$ ( $\text{cm}^2 \text{V}^{-1} \text{s}^{-1}$ )	ref
PDBPyTT	PyDPP	3.36	1.26	1 <sup>1</sup>
DPPPy-BT2CN	PyDPP	0.3	-	2 <sup>2</sup>
PDBPyDT2FBT	PyDPP	0.65	0.24	3 <sup>3</sup>
PDBPyBT	PyDPP	6.3	2.78	4 <sup>4</sup>
PPyDPP1-BT	PyDPP	1.05	0.86	5 <sup>5</sup>
PPyDPP1-4FBT	PyDPP	1.02	-	5 <sup>5</sup>
PPyDPP2-4FBT	PyDPP	2.45	-	5 <sup>5</sup>
PPyDPP1-4FTVT	PyDPP	1.19	-	5 <sup>5</sup>
PPyDPP2-4FTVT	PyDPP	1.35	-	5 <sup>5</sup>
PDPP[Py] <sub>2</sub> -T	PyDPP	0.63	-	6 <sup>6</sup>
PDPP[Py] <sub>2</sub> -TF2	PyDPP	0.15	-	6 <sup>6</sup>
PPyDPP-T	PyDPP	0.004	0.0008	7 <sup>7</sup>
PPyDPP-2FT	PyDPP	0.021	0.0003	7 <sup>7</sup>
PPyTDPP-TT	PyDPP	0.48	0.18	8 <sup>8</sup>
PPyTDPP-BT	PyDPP	0.08	0.55	8 <sup>8</sup>
PNDIBS	Se	0.07	-	9 <sup>9</sup>

PNDI-SVS	Se	2.4	-	10 <sup>10</sup>
PTDPPSe-SiC4	Se	3.07	6.16	11 <sup>11</sup>
PTDPPSe-SiC5	Se	4.34	8.84	11 <sup>11</sup>
PTDPPSe-SiC6	Se	2.2	3.97	11 <sup>11</sup>
P-24-DPPDBSE	Se	-	4.4	12 <sup>12</sup>
P-29-DPPDBSE	Se	-	12.04	12 <sup>12</sup>
PNBS	Se	8.3	1.6	13 <sup>13</sup>
PNBSF	Se	3	-	13 <sup>13</sup>
PDPPDTSE	Se	-	4.97	14 <sup>14</sup>
PCDSeBT	Se	-	0.001	15 <sup>15</sup>
PDPP(SE)- $\epsilon$ -C8C15	Se	2.25	12.25	16 <sup>16</sup>
eNDIBS	Se	0.24	-	17 <sup>17</sup>
PNBDO-ST5	Se	2.68	0.27	18 <sup>18</sup>
PNBDO-SS5	Se	0.012	0.0084	18 <sup>18</sup>
P(DPP-alt-DTBS <sub>2</sub> e)	Se	-	1.5	19 <sup>19</sup>

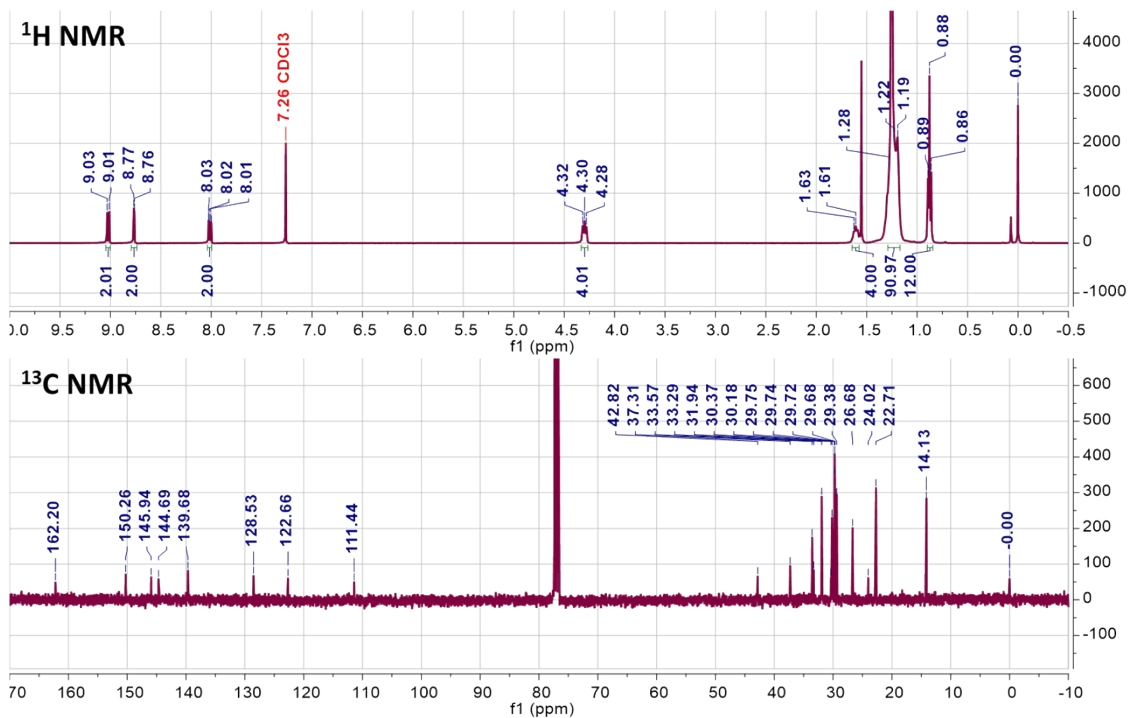


**Fig. S1** The <sup>1</sup>H and <sup>13</sup>C NMR spectroscopy of 5PyDPP.

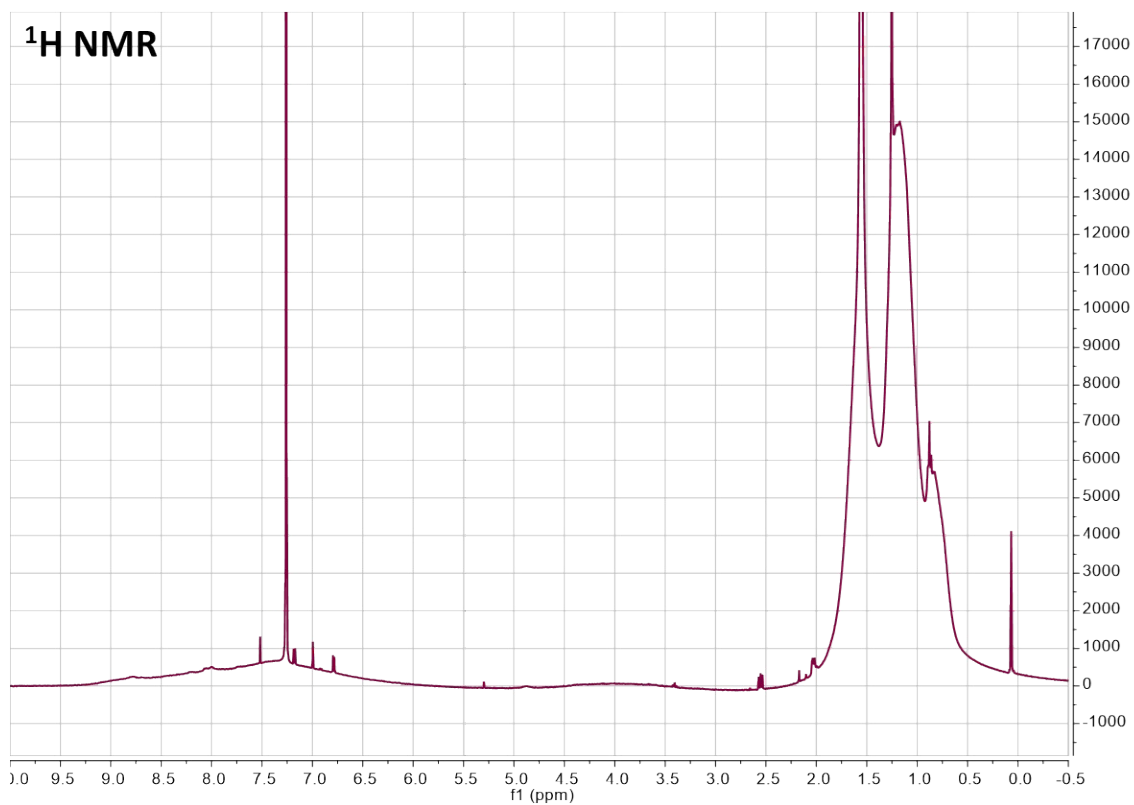


**Fig. S2** The <sup>1</sup>H NMR spectroscopy of P1.

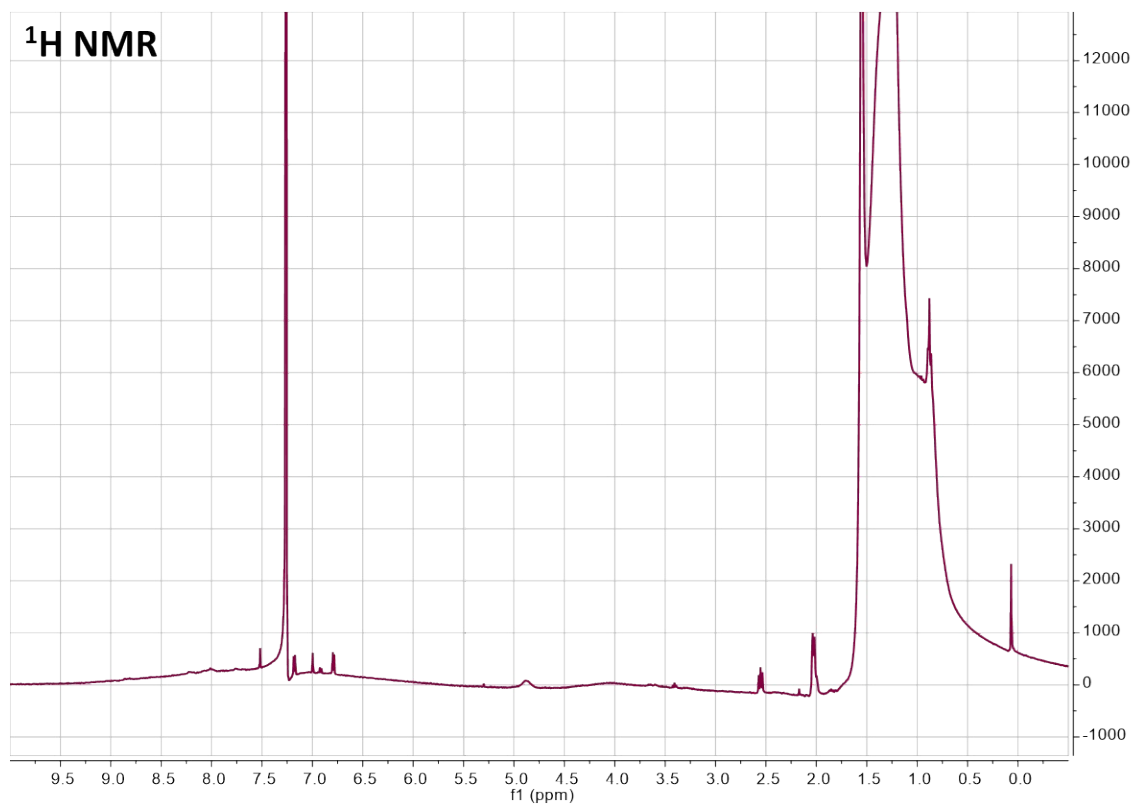


**Fig. S3** The <sup>1</sup>H NMR spectroscopy of P2.

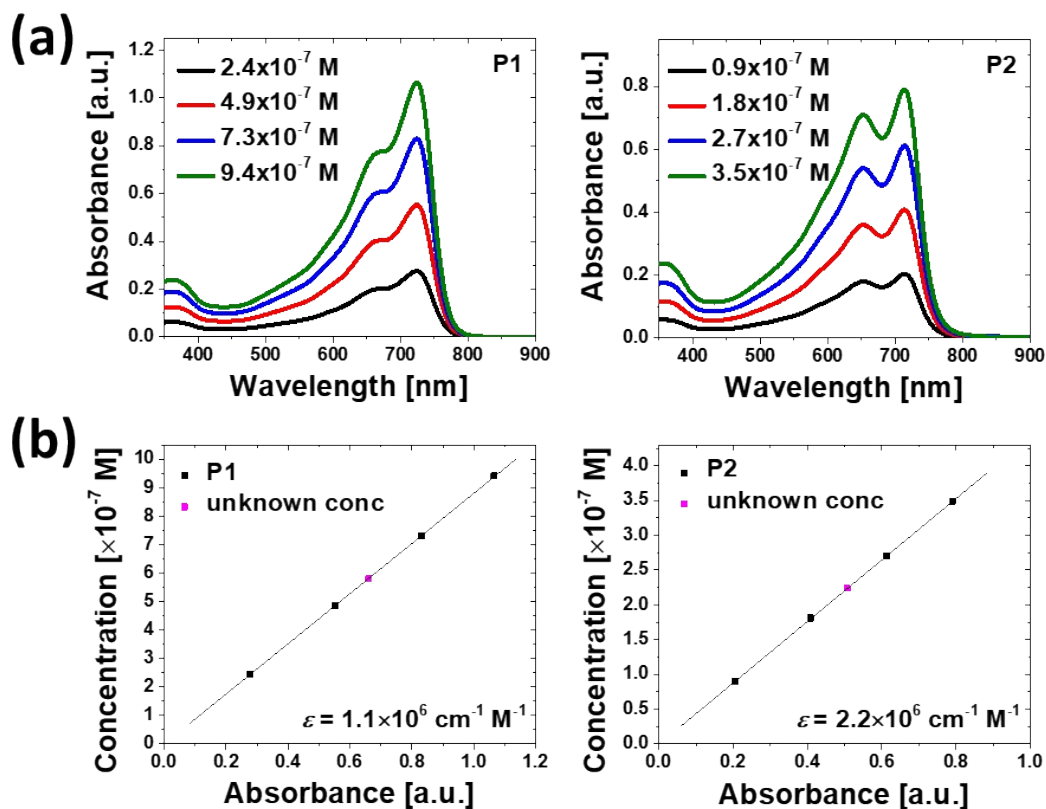


**Fig. S4** (a) UV-vis absorption spectra at different concentrations of the polymers in chlorobenzene and (b) calibration plots of the concentration of chlorobenzene-polymer solutions according to the measured absorbances at each  $\lambda_{\text{max}}$ .

**Table S2.** Solubility of the Polymers in Chlorobenzene (mg/mL).

	P1	P2
Solubility [mg/ mL]	5.80	2.24

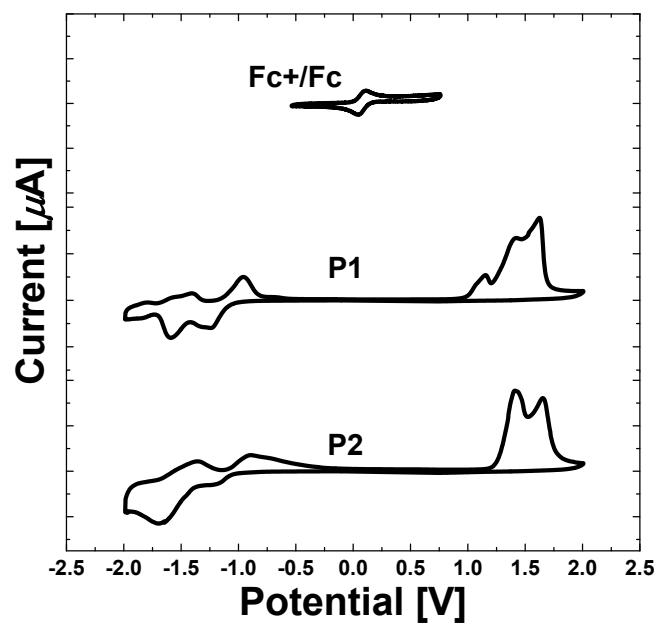


**Fig. S5** Cyclic voltammograms of the polymer films in  $n\text{-Bu}_4\text{NPF}_6/\text{CH}_3\text{CN}$  solution (scan rate,  $100\text{ mVs}^{-1}$ ).

**Table S3.** Calculated dipole moments and energy levels of the BT units by DFT.

	Vector			Dipole Moment [D]	$E_{\text{HOMO}}^{\text{DFT}}$ [eV]	$E_{\text{LUMO}}^{\text{DFT}}$ [eV]
	x	y	z			
<b>T1</b>	1.4123	3.4552	2.3629	4.4178	-5.11	-3.51
<b>T2</b>	1.4103	4.1109	1.1614	4.4986	-5.08	-3.49

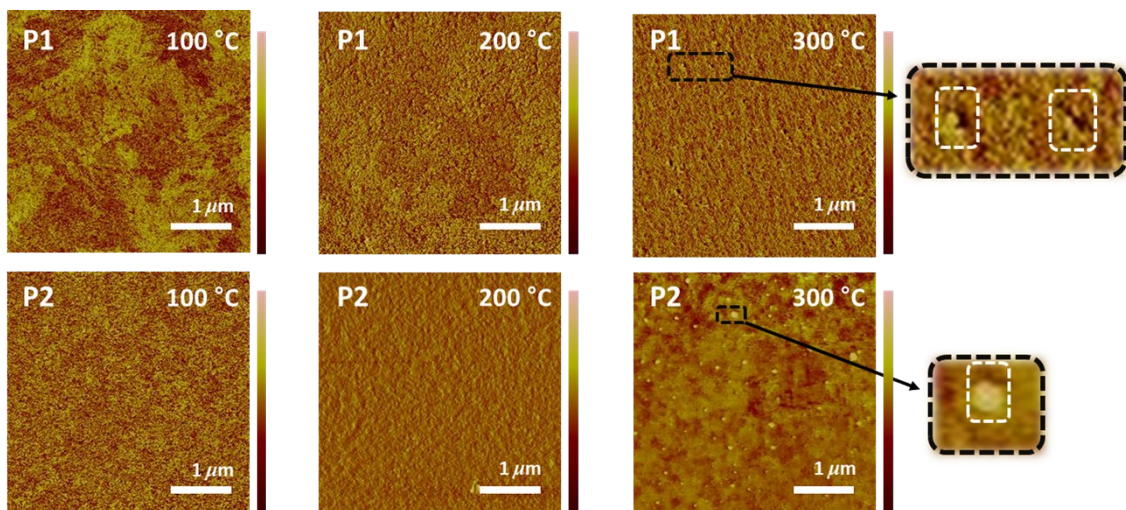


**Fig. S6** AFM phase images of annealed polymer films. The polymer films were formed by spin casting on SiO<sub>2</sub>/Si substrates.

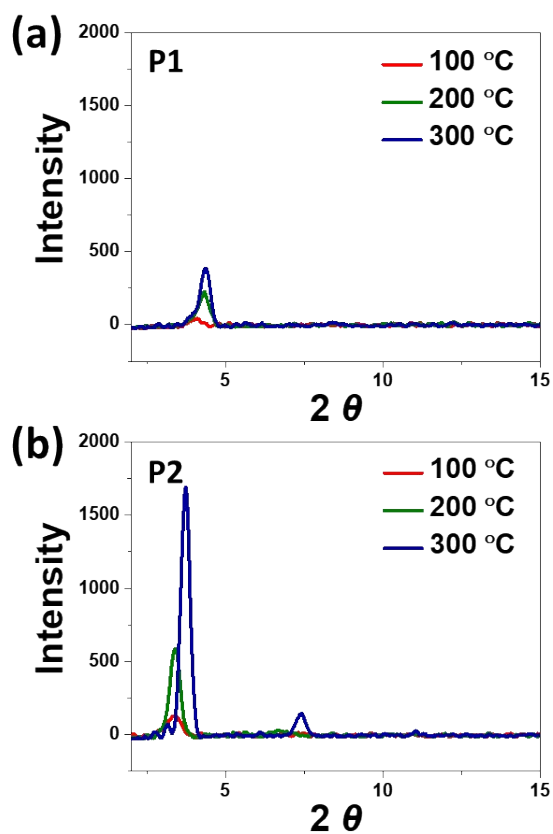


**Fig. S7** 1D out-of-plane XRD patterns of spin-casted (a) P1 and (b) P2 films on SiO<sub>2</sub> substrates at different annealing condition.

**Table S4.** Crystallographic parameters of spin-cast polymer films obtained from XRD at different annealing condition.

polymer film	Temperature [°C]	$2\theta$ [°]	d-spacing [Å]
P1	100	4.115	21.46
	200	4.3429	20.33
	300	4.3718	20.20
P2	100	3.3305	26.51
	200	3.4173	25.83
	300	3.7355	23.63

**Table S5.** 2D-GIXD crystallographic parameters of spin-cast polymer films at different annealing conditions.<sup>a</sup>

Polymer film	$T_a$ [°C]	Lamellar spacing <sup>b</sup>			$\pi$ - $\pi$ spacing <sup>c</sup>		
		$q_z$ [Å <sup>-1</sup> ]	$d_z$ [Å]	$L_c$ [Å]	$q_{xy}$ [Å <sup>-1</sup> ]	$d_{xy}$ [Å]	$L_c$ [Å]
P1	As-cast	0.274	22.90	122.2	1.741	3.61	90.7
	100	0.284	22.15	162.6	1.747	3.60	108.3
	200	0.303	20.77	309.0	1.743	3.61	121.9
	300	0.311	20.22	387.1	1.738	3.62	136.0
P2	As-cast	0.230	27.36	167.1	1.758	3.57	150.3
	100	0.231	27.18	217.5	1.758	3.57	170.0
	200	0.232	27.06	242.5	1.754	3.58	182.5
	300	0.261	24.09	425.8	1.754	3.58	201.8

<sup>a</sup>The parameters were calculated from GIXD profiles; The parameters for <sup>b</sup>the lamellar spacing and <sup>c</sup>the  $\pi$ - $\pi$  spacing were derived from the peaks along  $q_z$  and  $q_{xy}$  axis, respectively.

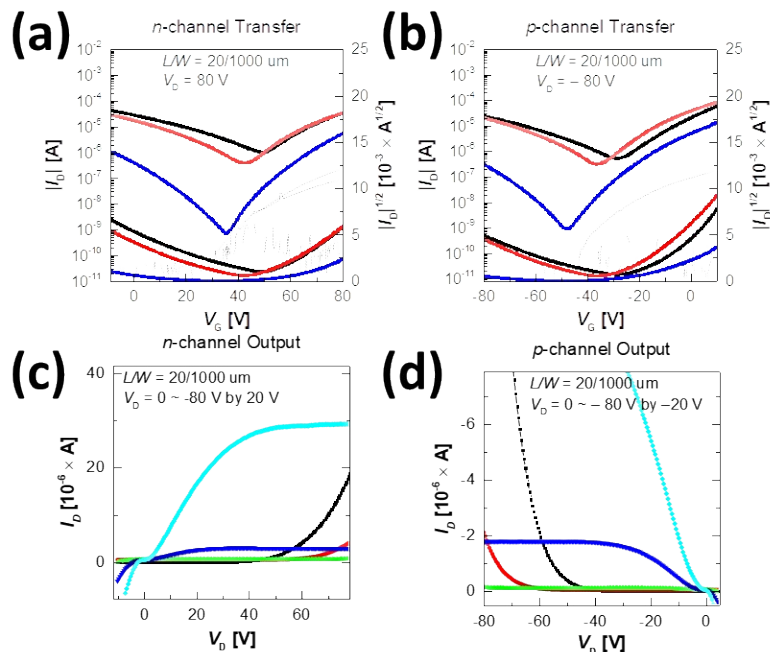


**Fig. S8** (a,b) Transfer and (c,d) output characteristics of the *n*-type and *p*-type devices of a low molecular weight P1 at different annealing conditions: 100 °C (black), 200 °C (red) and 300 °C (blue).

**Table S6.** Electrical characteristics of a low molecular weight P1 OFET Devices at different annealing conditions.

	$T_a$ [°C]	<i>n</i> -channel			<i>p</i> -channel		
		$\mu_e$ [cm <sup>2</sup> V <sup>-1</sup> s <sup>-1</sup> ]	$V_{th}$ [V]	$I_{on}$ / $I_{off}$	$\mu_e$ [cm <sup>2</sup> V <sup>-1</sup> s <sup>-1</sup> ]	$V_{th}$ [V]	$I_{on}$ / $I_{off}$
<b>P1</b> (16.2 kDa)	100	0.4 (± 0.1)	47 (± 8)	10	0.41 (± 0.2)	-26 (± 4)	10 <sup>2</sup>
	200	0.4 (± 0.02)	45 (± 2)	10 <sup>2</sup>	0.65 (± 0.03)	-35 (± 0.1)	10 <sup>2</sup>
	300	0.14 (± 0.03)	36 (± 1)	10 <sup>4</sup>	0.19 (± 0.01)	-35 (± 0.2)	10 <sup>4</sup>

4 devices for each condition were fabricated and used for mobility calculation.

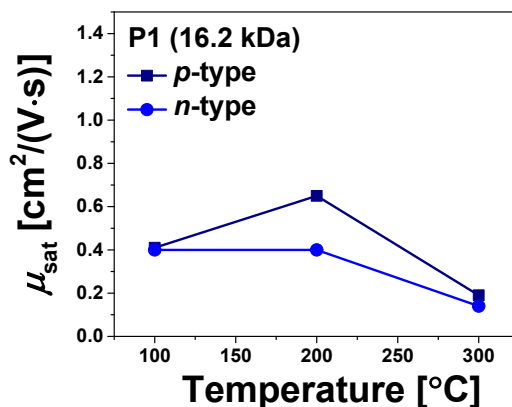


**Fig. S9** Hole and electron mobilities of a low molecular weight P1 at different annealing conditions.

**References**

- 1 B. Sun, W. Hong, H. Aziz, Y. Li, A Pyridine-Flanked Diketopyrrolopyrrole (DPP)-based Donor–Acceptor Polymer Showing High Mobility in Ambipolar and n-Channel Organic Thin Film Transistors, *Polym. Chem.*, 2015, **6**, 938-945.
- 2 Y. Sui, Y. Deng, Y. Han, J. Zhang, W. Hu, Y. Geng, n-Type Conjugated Polymers Based on 3,3'-Dicyano-2,2'-bithiophene: Synthesis and Semiconducting Properties, *J. Mater. Chem. C*, 2018, **6**, 12896-12903.
- 3 P. Li, L. Xu, H. Shen, X. Duan, J. Zhang, Z. Wei, Z. Yi, C.-a. Di, S. Wang, D–A1–D–A2 Copolymer Based on Pyridine-Capped Diketopyrrolopyrrole with Fluorinated Benzothiadiazole for High-Performance Ambipolar Organic Thin-Film Transistors, *ACS Appl. Mater. Interfaces*, 2016, **8**, 8620-8626.
- 4 B. Sun, W. Hong, Z. Yan, H. Aziz, Y. Li, Record High Electron Mobility of  $6.3 \text{ cm}^2\text{V}^{-1}\text{s}^{-1}$  Achieved for Polymer Semiconductors Using a New Building Block, *Adv. Mater.*, 2014, **26**, 2636-2642.
- 5 K. Guo, J. Bai, Y. Jiang, Z. Wang, Y. Sui, Y. Deng, Y. Han, H. Tian, Y. Geng, Diketopyrrolopyrrole-Based Conjugated Polymers Synthesized via Direct Arylation Polycondensation for High Mobility Pure n-Channel Organic Field-Effect Transistors, *Adv. Funct. Mater.*, 2018, **28**, 1801097.
- 6 C. J. Mueller, C. R. Singh, M. Fried, S. Huettner, M. Thelakkat, High Bulk Electron Mobility Diketopyrrolopyrrole Copolymers with Perfluorothiophene, *Adv. Funct. Mater.*, 2015, **25**, 2725-2736.
- 7 Z. Ni, H. Dong, H. Wang, S. Ding, Y. Zou, Q. Zhao, Y. Zhen, F. Liu, L. Jiang, W. Hu, Quinoline-Flanked Diketopyrrolopyrrole Copolymers Breaking through Electron Mobility over  $6 \text{ cm}^2 \text{ V}^{-1} \text{ s}^{-1}$  in Flexible Thin Film Devices, *Adv. Mater.*, 2018, **30**, 1704843.
- 8 G. Qiu, Z. Jiang, Z. Ni, H. Wang, H. Dong, J. Zhang, X. Zhang, Z. Shu, K. Lu, Y. Zhen, Z. Wei, W. Hu, Asymmetric Thiophene/Pyridine Flanked Diketopyrrolopyrrole Polymers for High Performance Polymer Ambipolar Field-Effect Transistors and Solar Cells, *J. Mater. Chem. C*, 2017, **5**, 566-572.
- 9 Y.-J. Hwang, G. Ren, N. M. Murari, S. A. Jenekhe, n-Type Naphthalene Diimide–Biselenophene Copolymer for All-Polymer Bulk Heterojunction Solar Cells, *Macromolecules*, 2012, **45**, 9056-9062.
- 10 M. J. Sung, A. Luzio, W.-T. Park, R. Kim, E. Gann, F. Maddalena, G. Pace, Y. Xu, D. Natali, C. de Falco, L. Dang, C. R. McNeill, M. Caironi, Y.-Y. Noh, Y.-H. Kim, High-Mobility Naphthalene Diimide and Selenophene-Vinylene-Selenophene-Based Conjugated Polymer: n-Channel Organic Field-Effect Transistors and Structure–Property Relationship, *Adv. Funct. Mater.*, 2016, **26**, 4984-4997.
- 11 J. Lee, A. R. Han, H. Yu, T. J. Shin, C. Yang, J. H. Oh, Boosting the Ambipolar Performance of Solution-Processable Polymer Semiconductors via Hybrid Side-Chain Engineering, *J. Am. Chem. Soc.*, 2013, **135**, 9540-9547.
- 12 I. Kang, H.-J. Yun, D. S. Chung, S.-K. Kwon, Y.-H. Kim, Record High Hole Mobility in Polymer Semiconductors via Side-Chain Engineering, *J. Am. Chem. Soc.*, 2013, **135**, 14896-14899.
- 13 Z. Zhao, Z. Yin, H. Chen, L. Zheng, C. Zhu, L. Zhang, S. Tan, H. Wang, Y. Guo, Q. Tang, Y. Liu, High-Performance, Air-Stable Field-Effect Transistors Based on Heteroatom-Substituted Naphthalenediimide-Benzothiadiazole Copolymers Exhibiting Ultrahigh Electron Mobility up to  $8.5 \text{ cm}^2 \text{ V}^{-1} \text{ s}^{-1}$ , *Adv. Mater.*, 2017, **29**, 1602410.
- 14 I. Kang, T. K. An, J.-a. Hong, H.-J. Yun, R. Kim, D. S. Chung, C. E. Park, Y.-H. Kim, S.-K. Kwon, Effect of Selenophene in a DPP Copolymer Incorporating a Vinyl Group for High-Performance Organic Field-Effect Transistors, *Adv. Mater.*, 2013, **25**, 524-528.
- 15 B. Kim, H. R. Yeom, M. H. Yun, J. Y. Kim, C. Yang, A Selenophene Analogue of

- PCDTBT: Selective Fine-Tuning of LUMO to Lower of the Bandgap for Efficient Polymer Solar Cells, *Macromolecules*, 2012, **45**, 8658-8664.
- 16 A.-R. Han, G. K. Dutta, J. Lee, H. R. Lee, S. M. Lee, H. Ahn, T. J. Shin, J. H. Oh, C. Yang,  $\epsilon$ -Branched Flexible Side Chain Substituted Diketopyrrolopyrrole-Containing Polymers Designed for High Hole and Electron Mobilities, *Adv. Funct. Mater.*, 2015, **25**, 247-254.
- 17 Y.-J. Hwang, N. M. Murari, S. A. Jenekhe, New n-Type Polymer Semiconductors based on Naphthalene Diimide and Selenophene Derivatives for Organic Field-Effect Transistors, *Polym. Chem.*, 2013, **4**, 3187-3195.
- 18 K. Shi, W. Zhang, Y. Zhou, C. Wei, J. Huang, Q. Wang, L. Wang, G. Yu, Chalcogenophene-Sensitive Charge Carrier Transport Properties in A–D–A''–D Type NBDO-Based Copolymers for Flexible Field-Effect Transistors, *Macromolecules*, 2018, **51**, 8662-8671.
- 19 J. S. Ha, K. H. Kim, D. H. Choi, 2,5-Bis(2-octyldodecyl)pyrrolo[3,4-*c*]pyrrole-1,4-(2*H*,5*H*)-dione-Based Donor–Acceptor Alternating Copolymer Bearing 5,5'-Di(thiophen-2-yl)-2,2'-biselenophene Exhibiting  $1.5 \text{ cm}^2 \cdot \text{V}^{-1} \cdot \text{s}^{-1}$  Hole Mobility in Thin-Film Transistors, *J. Am. Chem. Soc.*, 2011, **133**, 10364-10367.